Computer Simulation of Polymer Adsorption at Interfaces Using the Pivot Algorithm

Thomas C. Clancy and S. E. Webber*

Department of Chemistry and Biochemistry and Center for Polymer Research, University of Texas at Austin, Austin, Texas 78712

Received July 14, 1992; Revised Manuscript Received October 22, 1992

ABSTRACT: Monte Carlo simulations of self-avoiding polymers using the pivot algorithm have been employed to determine monomer distribution profiles, surface excess, and conformational variables for homopolymers and copolymers at solid–liquid and liquid–liquid interfaces in the dilute limit. A modified version of the pivot algorithm is used which allows the equilibrium between bulk and adsorbed polymers to be simulated. The segmental distribution profile and surface excess are determined as a function of χ, the energy increase associated with a monomer in an unfavorable environment. For the model employed, a diblock copolymer adsorbs more readily than an alternating copolymer at a liquid–liquid interface, while an alternating copolymer adsorbs more readily than a diblock at a solid–liquid interface. Simulations have also been carried out for homopolymers grafted to a surface at one end and by assigning energetic parameters to segment–segment ($\phi = -\epsilon_{segment}/kT$) and segment–surface ($\lambda = -\epsilon_{surface}/kT$) interactions. The effect of these parameters on the shape of the polymers and the number of segment–segment and segment–surface contacts was studied.

1. Introduction

Polymers at liquid–liquid and solid–liquid interfaces are of scientific and technological interest because of their various applications as surfactants and for colloidal stabilization. The properties of polymers at interfaces have been studied by various theoretical and experimental techniques. Much of the work has focused on the more concentrated regimes where brush formation occurs.[1,2] Monte Carlo simulations had previously been used only to determine the conformations of copolymers permanently affixed to an interface.[3,4] Halperin and Pincus[5] considered the distribution of homopolymers at a liquid–liquid interface using regular solution theory.

In this paper a modified version of the pivot algorithm[6] is used to determine the conformations of trapped diblock and alternating copolymers at liquid–liquid interfaces. We also use this method to compute the monomer density profiles and surface excess of copolymers at liquid–liquid and solid–liquid interfaces and of homopolymers at solid–liquid interfaces for the case in which the polymer can be distributed between the surface and the bulk solution. All simulations are performed in the dilute limit, in which polymers interacting only with solvent (or surface) are considered. The change in shape of the monomer distribution and the relative surface excess, $\Gamma_A/[A]$ (surface excess of monomer A/bulk concentration of monomer A), are determined as a function of χ, an energy parameter that describes the preference of a monomer unit for a particular environment.

Many investigators have studied the configurational behavior of adsorbed macromolecules using self-avoiding walks on lattices.[7–12] Most workers have assumed an adsorption energy for each segment in contact with the surface, which acts as a short-range attractive potential. In the present paper we examine an end-grafted polymer and have included a polymer–solvent interaction. We expected this latter quantity to be important primarily at low adsorption energies where the bulk of the polymer is in contact with the solvent and assumes a nearly random coil conformation. Under strongly adsorbing conditions, there is competition between the energetic stabilization when a polymer–wall contact is formed and the loss of entropy due to polymer collapse. Contrary to our expectation, we find that the solvent interaction continues to play an important role, even at the highest adsorption energies.

2. Method

2.1. The Pivot Algorithm. Polymer conformations are generated by the use of several variants of a modified pivot algorithm executed on a cubic lattice. The original pivot algorithm generates isotropic polymer conformations in a canonical ensemble.[6] The pivoting move consists of the random selection of a pivot point along the lattice-constrained polymer chain and the subsequent application of an appropriate symmetry operation to one of the two sections of the polymer which is bisected by the pivot point. (Here, the O_h point group corresponding to the cubic lattice is used.) The section on one specified side of the pivot point is arbitrarily chosen to be consistently pivoted with respect to the other section. We have applied this method to the simulation of intracoil energy transfer as a function of the solvent energy parameter ϕ,[13] and Johnson and Friesner[14] have applied this method to very large polymers. So far as we know this method has not been applied to a polymer in juxtaposition to an impenetrable surface or to a liquid–liquid interface. In the modified pivot algorithm used for the nongrafted polymer simulation, either one of the bisected polymer sections is allowed to pivot with respect to the other section. Alternatively, the entire polymer is pivoted about the selected pivot point. For simulation of bulk–interface equilibration, the entire polymer is permitted to move. Metropolis importance sampling and self-avoidance is applied for all cases.[15] The interface is set to lie on the plane determined by the equation $Z' = (X' + Y' - 1/2)$, where the primed coordinates lie along the cubic lattice. This is done so that it is possible for the alternating copolymer to achieve its minimum energy conformation. Figure 1 illustrates the geometry of the interface with respect to the cubic lattice.

We have also applied this algorithm to generate polymer conformations end-grafted to an impenetrable surface. In this case, the section of the bisected polymer which is not attached to the surface is consistently pivoted with respect to the other section. If the polymer intersects itself or the surface, the move is rejected. In addition, Metropolis biasing is applied.[15] In this case, the surface lies on the plane $Z' = 0$. The conformations generated from successive pivots are correlated since a given pivot only changes part of the polymer conformation. This may be characterized by calculating the correlation function for a given variable of interest, $\rho_A(i)$, defined by

$$\rho_A(i) = [\langle A(0)A(i)\rangle - \langle A\rangle^2]/[\langle A^2\rangle - \langle A\rangle^2] \quad (1)$$

0024-9297/93/2226-0628$04.00/0

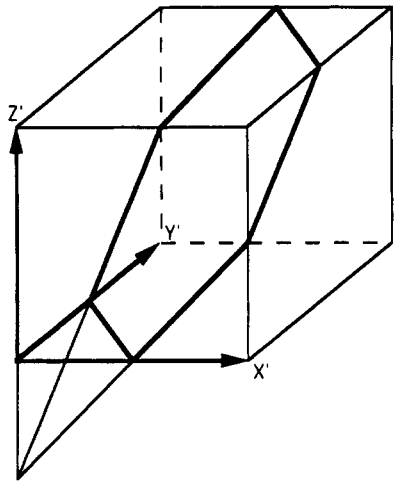

$Z' = X' + Y' - 1/2$

Figure 1. Illustration of the lattice coordinates used in this calculation.

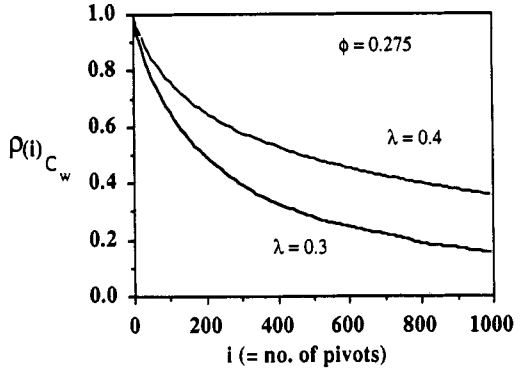

Figure 2. Plot of autocorrelation function vs number of pivots (i) for contacts with the wall (C_w) for $N = 50$ and energetic parameters indicated.

where

$$\langle A(0)A(i)\rangle = \sum_{k=1}^{M-i} A(k)A(k+i)/(M-i) \qquad (2)$$

In the calculation of the correlation function, the number of conformations, M, was usually 5×10^5 or 1×10^6 and the number of successive pivot moves, i, varied from 1000 to 6000. The behavior of the correlation function depends strongly on the variable examined as well as the energetic parameters. To obtain statistically independent samples from this dynamic algorithm, it is necessary to determine the correlation time, (τ), for variables of interest, where τ is the number of pivots required to reduce the correlation function to a value of $1/e$. It has been shown that 2τ pivots must be executed to arrive at a statistically independent conformation for a given variable.[6] In both the end-grafted and trapped copolymer simulations, the variable C_w, the average number of contacts with the wall, usually had the longest correlation time. The behavior of $\rho(i)_{C_w}$ is illustrated in Figure 2. At high ϕ values and low λ values, however, the average number of segmental contacts, C, had a slightly longer correlation time. Table I lists the longer of the C and C_w correlation times for solvent and surface energetic parameters ϕ and λ (see section 2.5 for the definition of these quantities). Conformational variables were determined according to this method for end-grafted polymers and trapped copolymers at liquid–liquid interfaces but not for any of the other cases. In the bulk–interface equilibrium calculations, all conformations satisfying the self-avoidance (and impenetrable wall avoidance) and Metropolis biasing criteria were accepted into the ensemble. In that case, the statistical validity of the calculation was assessed by the standard deviation of the bulk solution concentration.

2.2. The End-Grafted Case. In our calculation we begin by starting the initial homopolymer conformation as rodlike and perpendicular to the surface. Approximately 10τ pivots are executed to thermalize the polymer. The pivoting continues, and conformations are accepted into the ensemble at pivoting intervals of approximately 2τ or larger. This procedure is continued until the ensemble contains 5000 conformations. Four equivalent ensembles of 5000 conformations, each started with a different seed for the random number generator, are generated, and the averages and standard deviations are calculated. For all calculations 50 monomer units were used.

Since there are two criteria for pivoting to a new conformation, we can consider two acceptance fractions for pivot moves. Acceptance fraction f_1 corresponds to the fraction of pivots which are accepted on the basis of nonintersection of the new conformation with either the surface or itself. The second acceptance fraction, f_2, corresponds to the fraction of pivots which fulfill the above criterion as well as the energetic criterion imposed by the Metropolis importance sampling method. Table I lists both fractions at the various ϕ and λ values.

Table I
Correlation Time for C and C_w and Acceptance Fraction for Pivot Algorithm Calculation as a Function of ϕ and λ for an End-Grafted Chain of 50-Segment Length

ϕ	λ	$\tau(C_w)$	$\tau(C)$	f_1[a]	f_2[b]	cpu time,[c] s
0.0	0.0	45		0.50	0.50	62
0.0	0.1	49		0.49	0.47	93
0.0	0.2	72		0.47	0.42	139
0.0	0.3	185		0.43	0.34	252
0.0	0.4	425		0.39	0.25	660
0.0	0.6	1733		0.34	0.16	2516
0.15	0.0	31		0.48	0.44	64
0.15	0.1	41		0.47	0.42	64
0.15	0.2	70		0.45	0.37	95
0.15	0.3	177		0.41	0.30	251
0.275	0.0		36	0.46	0.37	63
0.275	0.1		36	0.44	0.35	65
0.275	0.2	83		0.42	0.31	127
0.275	0.3	164		0.38	0.24	257
0.275	0.6	2368		0.31	0.12	3163
0.35	0.0		51	0.43	0.32	65
0.35	0.1		55	0.42	0.30	79
0.35	0.2	80		0.39	0.26	130
0.35	0.3	179		0.36	0.21	264

[a] Fraction of pivots that are nonintersecting. [b] Fraction of pivots that simultaneously are nonintersecting and satisfy the Metropolis criterion. [c] Time required to obtain 5000 statistically independent conformations.

2.3. The Case of a Polymer Trapped at a Liquid–Liquid Interface. In the liquid–liquid copolymer case, the simulation is carried out in two distinctive ways wtih two different objectives. In the first type of simulation, the purpose was to compare the shapes of adsorbed copolymers to that of an isotropic polymer. A sufficiently high χ value was used to effectively anchor the copolymer at the interface (see later discussion) and geometric variables such as the radius of gyration squared $\langle R_g^2\rangle$ and the end-to-end distance squared $\langle S^2\rangle$ were computed. The autocorrelation times, (τ_i), of these variables determined the intervals at which conformations were accepted into an ensemble. Four ensembles of 5000 conformations were generated for diblock and alternating copolymers with 50 monomers. In addition, the monomer distribution profiles of both types of monomer were calculated as a function of distance from the interface (Z). This type of simulation was applied only to the copolymer at the liquid–liquid interface.

2.4. Equilibration between Bulk and Adsorbed Polymer. In this second type of simulation, performed for both liquid–liquid and solid–liquid cases, the polymer was not attached to the interface and the monomer distribution profile and surface excess were determined. To accomplish this, an additional Monte Carlo translation of the entire polymer with respect to the interfacial plane over a limited number of lattice points was added. The polymer is constrained to remain in the vicinity of the interface by means of a reflection of the polymer toward the interface if any segment goes beyond 400 lattice points from the interface. The polymer is initially placed near or at the interface. Thermalization is achieved by 50 000 Monte Carlo steps, after

Table II
Conformational Properties of Copolymers Trapped at the Liquid–Liquid Interface or in Isotropic Solution (N = 50)

property	alternating[a] (χ = 2.0)	diblock[a] (χ = 1.0)	isotropic[a] (χ = 0)
$\langle R_g^2\rangle_\parallel$	22.54 (0.767)	10.18 (1.34)	12.22 (1.03)[b]
$\langle R_g^2\rangle_\perp$	0.5431 (0.651)	13.12 (0.702)	6.090 (0.515)[b]
$\langle R_g^2\rangle$	23.09 (0.743)	23.30 (0.886)	18.31 (0.720)
$\langle S^2\rangle$	159.6 (1.584)	157.5 (1.533)	116.6 (0.699)
$\langle C\rangle$	2.261 (0.072)	2.281 (0.104)	2.310 (0.145)
$\langle C_w\rangle$	0.7254 (0.033)	0.07670 (0.703)	

[a] The values in parentheses are the percent standard deviation of the mean. [b] In the isotropic case, the average value of the minimum component of $\langle R_g^2\rangle$ is defined as $\langle R_g^2\rangle_\perp$, while the sum of the other two components is defined as $\langle R_g^2\rangle_\parallel$.

which the monomer distribution with respect to the interface is sampled over the 200 lattice points about the interface ($-100 < Z < 100$). The distribution functions discussed later imply that this sampling region is adequate to avoid any "edge effects". Larger regions were used, and this size was determined to be adequate for $N = 50$. Between 5×10^5 and 5×10^6 conformations are generated to produce the final interfacial distribution profile.

2.5. Energetic Parameters. The copolymer consists of A- and B-type segments and is placed near the sharp interface of two immiscible liquids A and B or at the solid–liquid interface. The conformations are assigned energetic values according to the following scheme: Type A monomers in liquid A and type B monomers in liquid B are at the zero of energy. Type A monomers in liquid B and type B monomers in liquid A are assigned the energy χ for each monomer. The copolymers are therefore at their minimum energy configuration when straddling the interface. In the case of the copolymer at a solid surface, an impenetrable wall is placed at the plane defined by $Z' = (X' + Y' - 3/2)$. In this case, type B monomers that do not lie on lattice sites located between the planes $Z' = (X' + Y' - 3/2)$ and $Z' = (X' + Y' - 1/2)$ are assigned the energy χ for each monomer and type A monomers that do lie between these planes are assigned the energy χ for each monomer.

For the end-grafted homopolymer two energetic parameters were used, the segment–segment interaction energy, $\phi = -\epsilon_1/kT$, and the energy of adsorption, $\lambda = -\epsilon_2/kT$. ϵ_1 is the difference in energy between the segment–segment contact and segment–solvent and solvent–solvent contact, while the energy of adsorption, λ, is the energy difference between a segment–surface bond and the energy required to break a solvent–surface and segment–solvent contact

$$\epsilon_1 = \epsilon_{\text{segment–segment}} - (\epsilon_{\text{segment–solvent}} + \epsilon_{\text{solvent–solvent}})$$

$$\epsilon_2 = \epsilon_{\text{segment–surface}} - (\epsilon_{\text{segment–solvent}} + \epsilon_{\text{solvent–surface}}) \qquad (3)$$

such that the total energy of the ith polymer is given by

$$\epsilon_{\text{total}} = c_i\epsilon_1 + c_w{}^i\epsilon_2 \qquad (4)$$

where c_i and $c_w{}^i$ are the total number of segment–segment and segment–surface contacts for the ith member of the ensemble.

Four values of ϕ were used: $\phi = 0$ (the hard-sphere model), $\phi = 0.15$, $\phi = 0.275$ (the Flory θ-point), and $\phi = 0.35$ (a poor solvent). At high values of ϕ nonbonded chromophore contacts are weighted more heavily, such that compact coils contribute more to the ensemble average. Likewise, at high values of λ those conformations with a large number of wall contacts contribute heavily to the average. Adsorption is favored for negative values of ϵ_2 and was varied from $\epsilon_2 = -0.6kT$ to $0.0kT$. The solvent affects the adsorption both by interacting with the polymer directly and by indirectly competing with the polymer for the surface.

3. Results and Discussion

3.1. Liquid–Liquid Interface. 3.1.1. Conformations of Polymers Trapped at the Interface. Table II shows the geometric variables for a diblock and an alternating copolymer fixed at the surface by sufficiently high χ values along with the values for an isotropic coil (the requirements to trap these polymers at an interface will be discussed later). The adsorbed polymers are larger than an isotropic polymer generated with the same algorithm. For example, the average end-to-end distance squared ($\langle S^2\rangle$) increases by 35% and 37%, respectively, for the diblock and alternating copolymers. Similarly, the radius of gyration squared ($\langle R_g^2\rangle$) increases by 27% and 26% and the number of nonbonding segmental contacts ($\langle C\rangle$) decreases by 1% and 2% for the diblock and alternating copolymers, respectively. As expected, the presence of the interface causes the diblock copolymer to stretch out perpendicularly with respect to the interface. Likewise, the alternating copolymer tends to lie in the interfacial plane as evidenced by the low value of the perpendicular component of $\langle R_g^2\rangle$. The number of segmental contacts with the interface ($\langle C_w\rangle$) is also dramatically different for the two cases, as would be expected.

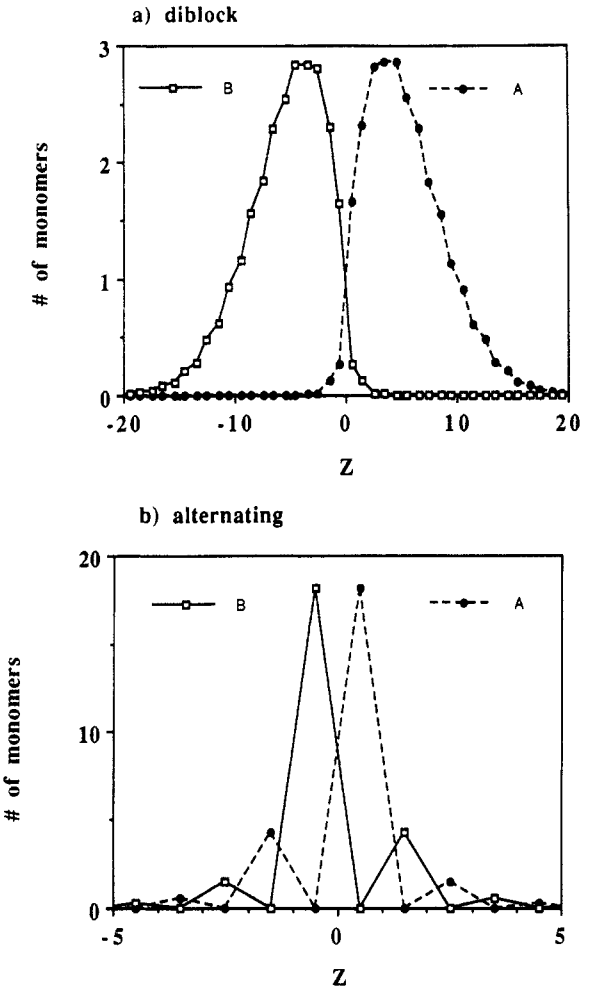

Figure 3. Normalized distribution of A and B segments with respect to the liquid–liquid interface (at $Z = 0$) (a) for a trapped diblock copolymer (χ = 1.0) and (b) for a trapped alternating copolymer (χ = 2.0).

Figure 3 shows the monomer distribution profiles. The alternating copolymer requires a higher χ value ($\chi \approx 2.0$) than the diblock ($\chi \approx 1.0$) to be irreversibly bound to the interface (see later discussion). The diblock monomer distributions have their maxima at 3–5 lattice units (lu) from the interface, declining to half that value at the 9th lattice point from the interface. The alternating copolymer monomer distributions have their maxima adjacent to the interface, with approximately 70% of the monomers at this position.

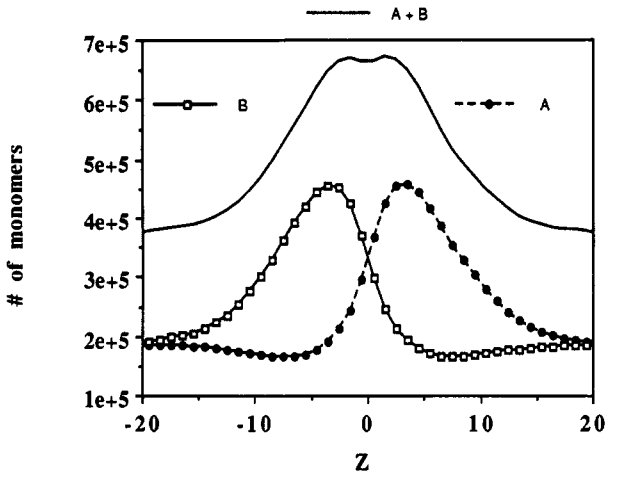

Figure 4. Distribution of monomer units with respect to the liquid–liquid interface at $Z = 0$ for a diblock copolymer ($\chi = 0.1$, $N = 50$).

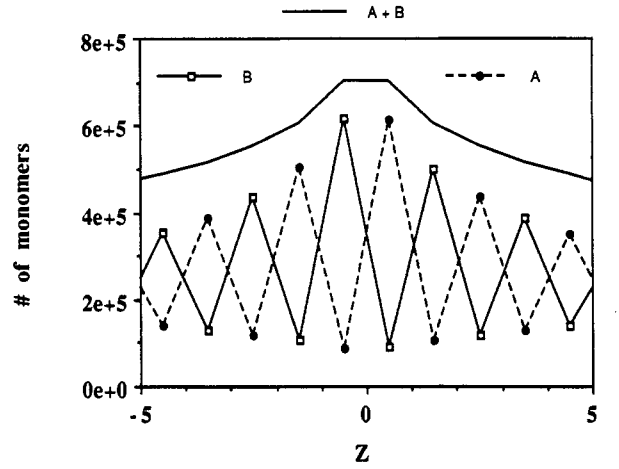

Figure 5. Distribution of monomer units with respect to the liquid–liquid interface at $Z = 0$ for an alternating copolymer ($\chi = 0.4$, $N = 50$).

3.1.2. Bulk-Interface Equilibrium. Figure 4 shows the individual (A, B) monomer distribution profiles and the total (A + B) monomer distribution profile for a diblock copolymer of length 50 with $\chi = 0.1$ (note that this distribution is not normalized as was the case for Figure 3). In this case, the copolymer is not trapped at the interface, but there remains an excess of copolymer in this region due to the interaction of the monomers with the two solvents. The distribution of the excess monomer density above the bulk concentration baseline is similar to the fixed diblock profile. In this case, the monomer density immediately adjacent to the "wrong" side of the interface decreases below the bulk value, which is a correlation effect.

Figure 5 shows the monomer distribution profiles for a perfectly alternating copolymer (ABABAB) of length 50 with $\chi = 0.4$. The profiles are similar to those of the fixed alternating copolymer, with the maximum located adjacent to the interface. A higher χ value is required in the alternating case to achieve a surface excess comparable to that of the diblock case.[16]

Figure 6 is a plot of the monomer distribution profiles at low χ ($\chi = 0.1$) for the alternating copolymer ($N = 50$). The total monomer distribution profile (A + B) is essentially flat, while that of A or B continues to oscillate, implying that the polymer configurations may be influenced by the presence of the interface even though there is little or no surface excess of polymer. We have not examined this phenomenon in detail at the present time.

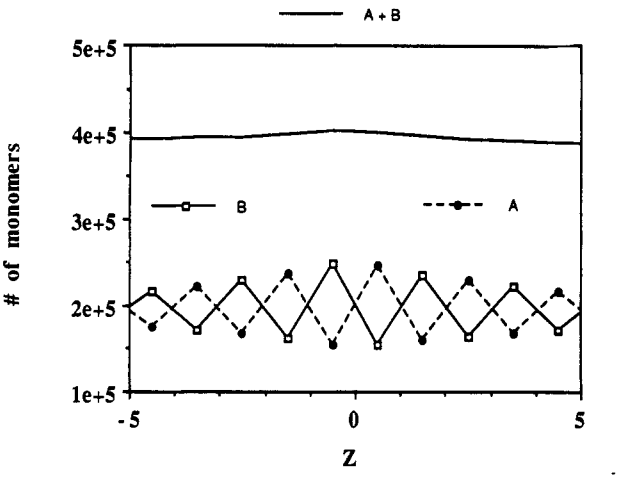

Figure 6. Distribution of monomer units with respect to the liquid–liquid interface at $Z = 0$ for an alternating copolymer ($\chi = 0.1$, $N = 50$).

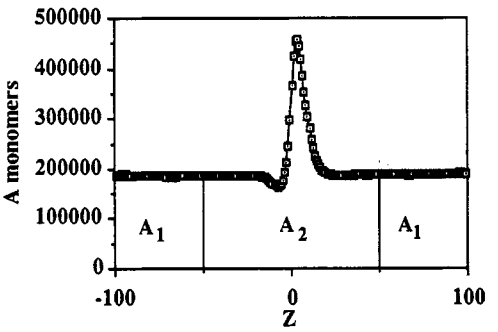

Figure 7. Illustration of the computation of $\Gamma_A/[A]$. A_i refers to the areas under the appropriate sections of the curve.

The surface excess (Γ) of an adsorbed species can be used with the Gibbs equation to compute the interfacial surface tension, (γ)

$$\frac{-1}{RT}\frac{d\gamma}{dc} = \frac{\Gamma}{c} \tag{5}$$

where c is the bulk concentration for an ideal solution. Since we are in the infinitely dilute region, in principle we can compute the limiting interfacial surface tension between liquids as a function of polymer type and energetic parameters. For the present purposes we merely examine the surface excess with respect to either A or B monomer or for the total monomer population as a qualitative measure of relative surface activity. Figure 7 demonstrates how we calculate the surface excess ($A_2 - 2A_1$) and the bulk concentration of monomer ($2A_1$). The statistical validity is assessed by considering the standard deviation of the height of the profile in the bulk solvent region ($-100 < Z < -50$) $\cup$ ($100 > Z > 50$) for equivalent ensembles.

Figure 8 shows the surface excess, (Γ_A), divided by the bulk concentration, ([A]), as a function of the parameter χ for the diblock and alternating copolymers with $N = 50$. Over the χ range plotted, this quantity appears to increase approximately exponentially with χ (for both polymer types), although as χ approaches zero the surface excess must also approach zero. Also, at some value of χ (approximately 1.0 in the diblock case and 2.0 in the alternating case), the copolymer becomes essentially localized at the interface, in which case $\Gamma_A/[A]$ approaches infinity.

3.2. Solid–Liquid Interface. 3.2.1. End-Grafted Homopolymer. All calculations were done for polymers with 50 segments. Some representative values of conformational quantities are presented in Table III. The

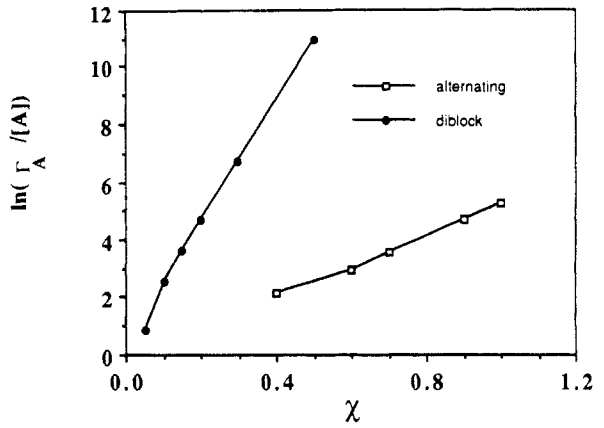

Figure 8. Semilogarithmic plot of $\Gamma_A/[A]$ vs χ for diblock and alternating copolymers.

Table III
Conformational Results for End-Grafted Polymer

Results for $\lambda = 0$ or for Isotropic Solution

ϕ	$\langle S^2\rangle$	$\langle R_g^2\rangle$	$\frac{\langle S^2\rangle}{\langle R_g^2\rangle}$	$\langle C_w\rangle$	$\langle C\rangle$
0	135 (±0.97%)	19.0 (±0.38%)	7.11	0.0789 (±2.1%)	2.304 (±0.15%)
0.15	120 (±0.52%)	17.1 (±0.25%)	7.02	0.0811 (±0.90%)	2.406 (±0.060%)
0.275	103 (±0.59%)	14.9 (±0.44%)	6.91	0.0835 (±1.3%)	2.537 (±0.068%)
0.35	93.1 (±1.1%)	13.6 (±0.67%)	6.85	0.0869 (±1.2%)	2.637 (±0.097%)
0[a]	116 (±0.31%)	18.0 (±0.19%)	6.43	*b*	2.313 (±0.22%)
0.15[a]	99.2 (±0.30%)	15.8 (±0.32%)	6.28	*b*	2.424 (±0.60%)
0.275[a]	82.4 (±0.39%)	13.5 (±0.20%)	6.10	*b*	2.560 (±0.27%)
0.35[a]	70.4 (±0.44%)	11.9 (±0.38%)	5.92	*b*	2.674 (±0.62%)

Results for $\phi = 0.275$

λ	$\langle S^2\rangle$	$\langle R_g^2\rangle$	$\frac{\langle S^2\rangle}{\langle R_g^2\rangle}$	$\langle C_w\rangle$	$\langle C\rangle$
0	103 (±0.59%)	14.9 (±0.44%)	6.91	0.0835 (±1.3%)	2.537 (±0.068%)
0.10	100 (±1.2%)	14.7 (±0.51%)	6.80	0.113 (±1.3%)	2.544 (±0.13%)
0.20	97.9 (±0.65%)	14.7 (±0.76%)	6.66	0.170 (±0.70%)	2.557 (±0.15%)
0.30	96.4 (±1.1%)	14.75 (±0.60%)	6.54	0.268 (±0.38%)	2.576 (±0.16%)
0.60	133 (±0.90%)	19.8 (±0.67%)	6.72	0.665 (±0.71%)	2.550 (±0.15%)

[a] For isotropic solution. [b] Not applicable for isotropic solution.

average end-to-end distance squared ($\langle S^2\rangle$) and mean squared radius of gyration ($\langle R_g^2\rangle$) as a function of adsorption energies are plotted for various solvent interaction energies ϕ in Figure 9. (See Dean and Webber[17] for other ϕ values.) Generally, the better polymer solvents (smaller ϕ) resulted in larger values of $\langle R_g^2\rangle$ and $\langle S^2\rangle$, reflecting more loosely coiled configurations, as expected. The value of $\langle S^2\rangle/\langle R_g^2\rangle$ increases from ca. 6 for the isotropic coil at $\phi = 0.275$ (θ-condition) to 6.5–7.1 in the presence of the wall for the same ϕ values. The anisotropic effects due to the wall are illustrated by the radius of gyration parallel ($\langle R_g^2\rangle_\parallel$) and perpendicular ($\langle R_g^2\rangle_\perp$) to the surface (Figure 10).[18] $\langle R_g^2\rangle_\parallel$ and $\langle R_g^2\rangle_\perp$ are modified by the wall for all λ, while $\langle R_g^2\rangle$ is affected only slightly for $\lambda < 0.4$. The effect of the attractive wall is to flatten the polymer coil, making it more two-dimensional. In all dimensional comparisons with a coil in isotropic solution,

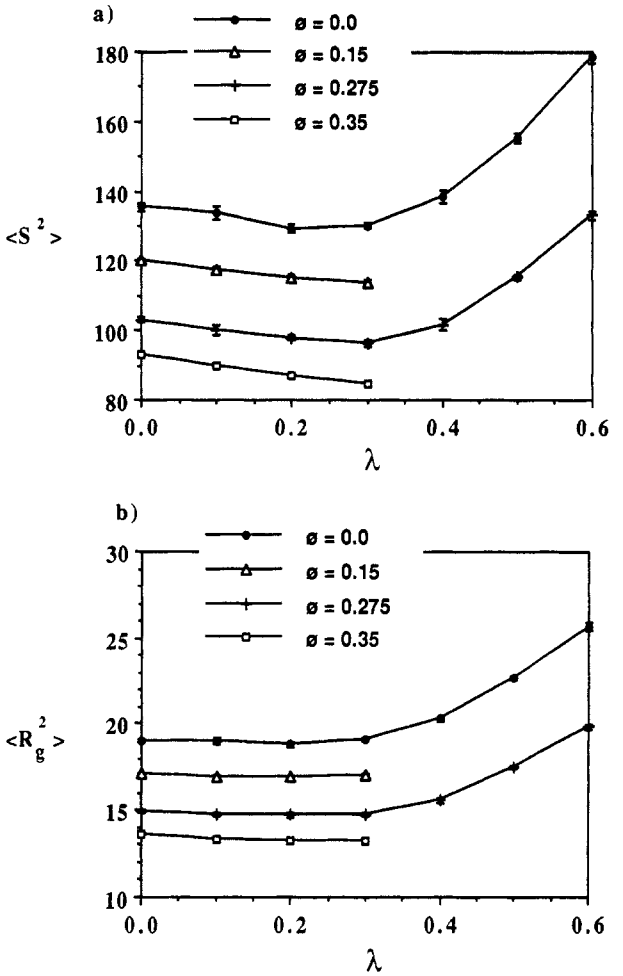

Figure 9. (a) $\langle S^2\rangle$ and (b) $\langle R_g^2\rangle$ as a function of λ for ϕ values indicated. Error bars, which represent the standard deviation for four ensembles each with 5000 polymer coils, are difficult to see on this scale.

the coil attached to a wall appears to be larger. This agrees with the recent calculation of Hahn and Kovac for terminally attached polymers with excluded volume.[19]

In Figure 11a we have plotted the average number of all contacts, bonded and nonbonded, per chromophore ($\langle C\rangle$) as a function of λ for several ϕ values. Generally more contacts are formed in poor solvents ($\phi = 0.35$) than in good solvents ($\phi = 0$), reflecting the increased coil compactness in the former case. The changes in $\langle C\rangle$ with increasing adsorption energy, λ, are relatively minor compared to the effect of ϕ.

The average number of wall contacts per chromophore ($\langle C_w\rangle$) is equivalent to the fraction of polymer adsorbed and is plotted as a function of λ for all ϕ values in Figure 11b. The fraction of adsorbed polymers is essentially independent of solvent strength but very sensitive to λ. When the energy of adsorption is zero, ~8% of the chromophores are located on the wall,[20] while at $\lambda = 0.60$, ~64% of the chromophores are in contact with the wall. Apparently the solvent strength (ϕ) does not affect the fraction of polymer adsorbed but does affect the average shape of the coils on the basis of the dependencies shown in Figures 9 and 10. Figure 12 shows the monomer distribution profiles for end-grafted chains with several different values of λ with $\phi = 0.0$.

These conformational changes can be described as occurring in two phases. In the first phase, from $\lambda = 0$ to 0.25, the average shape of the polymer remains essentially constant according to $\langle R_g^2\rangle$ and $\langle C\rangle$, but the radii of gyration relative to the surface, $\langle R_g^2\rangle_\parallel$ and $\langle R_g^2\rangle_\perp$, are

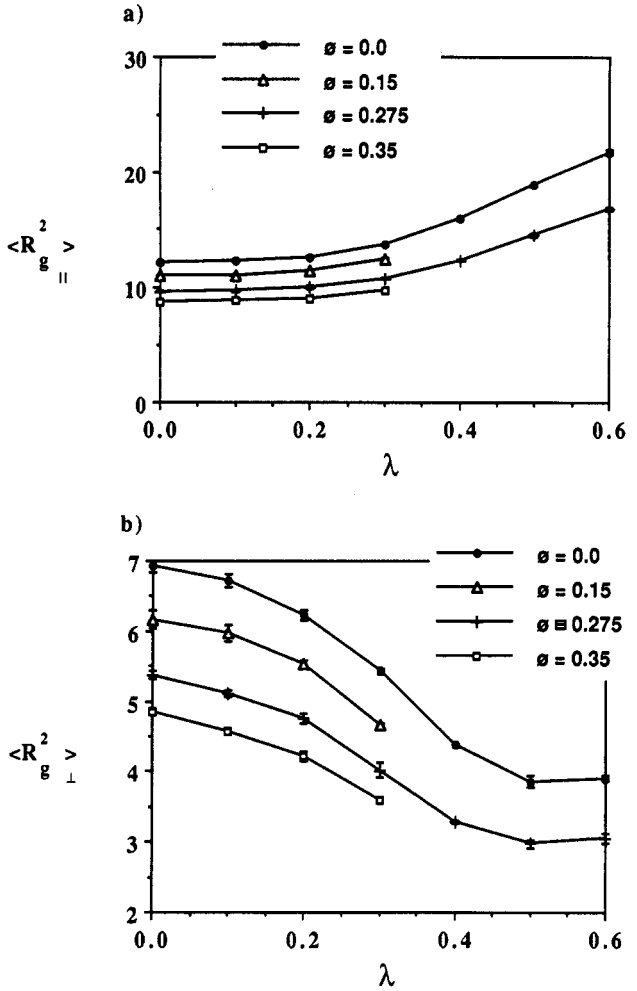

Figure 10. (a) $\langle R_g^2\rangle_\parallel$ and (b) $\langle R_g^2\rangle_\perp$ as a function of λ for ϕ values indicated.

modified slightly. This corresponds to the major axis of the ellipsoidal coils aligning themselves along the surface, while the coil retains its overall shape. Some similar results have been reported in earlier calculations. McCrackin[21] reported a critical value of the adsorption energy of 0.25, below which the fraction of segments on the surface was small. Similarly, Rubin[22] obtained a critical value of 0.212 for λ, below which the fraction of segments on the surface was zero. For larger values of λ the average shape of the coils changes, as reflected by the increase in $\langle R_g^2\rangle$ and $\langle R_g^2\rangle_\parallel$ which represents an elongation of the coils parallel to the surface. The largest increase of $\langle C\rangle$ with λ is much less than the differences between different ϕ values. $\langle R_g^2\rangle_\perp$ sharply decreases and $\langle C_w\rangle$ increases as the coils strongly adsorb to the surface.

3.2.2. Analysis of the Ensemble Sampling Using the Pivot Algorithm. It is possible to obtain data for different λ or ϕ values from one simulation by applying a reweighting technique. The simulation is performed as usual for some choice of λ and ϕ. In addition, the energy of each conformation is assessed with a secondary set of λ and ϕ parameters. The variables of the conformation are placed into an independent ensemble and are reweighted according to the Boltzmann distribution. Thus, a conformation generated in a simulation with the energetic parameters λ_1 and ϕ_1 would be reweighted in the secondary ensemble by applying a weighting factor, w_i, to the conformation according to the equation

$$w_i = \exp(c_w{}^i\lambda_1 + c_i\phi_1)/\exp(c_w{}^i\lambda_2 + c_i\phi_2) \qquad (6)$$

where c_i is the number of internal contacts, $c_w{}^i$ is the number of wall contacts for the polymer conformation,

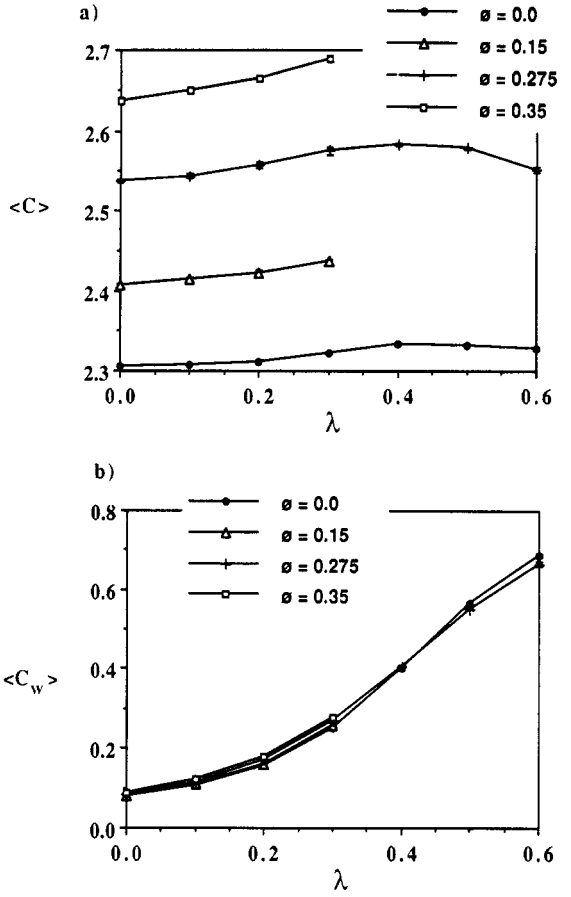

Figure 11. (a) $\langle C\rangle$ and (b) $\langle C_w\rangle$ as a function of λ for ϕ values indicated. Error bars are as in Figure 9. Note that the minimum possible values of $\langle C\rangle$ and $\langle C_w\rangle$ would be 1.96 and 0.02, respectively (one-dimensional chain perpendicular to the surface).

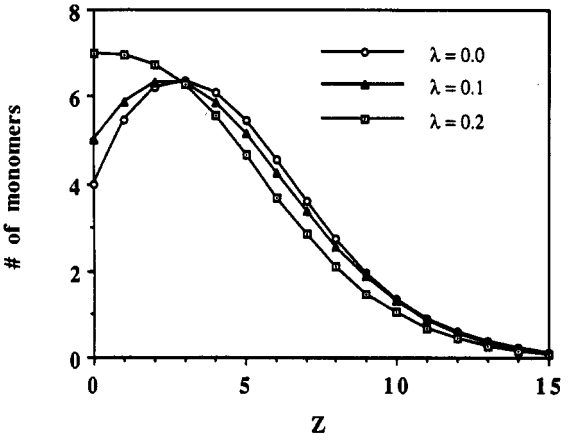

Figure 12. Monomer distributions for end-grafted homopolymers (N = 50) with respect to the wall at Z = 0, ϕ = 0, and λ = 0.0, 0.1, and 0.2.

and λ_2 and ϕ_2 are the new set of energetic parameters. Any given variable, A, is then averaged according to the equation

$$\langle A\rangle = \sum_{i=1}^{N} w_i A / \sum_{i=1}^{N} w_i \qquad (7)$$

If our sampling of the ensemble of polymer conformations were unbiased, then this approach would be exact. Figure 13 shows results for $\langle R_g^2\rangle_\perp$ and $\langle R_g^2\rangle_\parallel$ using this technique. The simulation is run initially at the values λ_1 = 0.2 and ϕ_1 = 0.0. The reweighting method is applied to generate six additional ensembles at ϕ_2 = 0.0 and λ_2 from 0 to 0.6. The same trends are produced in all cases, and when the difference between λ_1 and λ_2 is less than ca. 0.1–0.2,

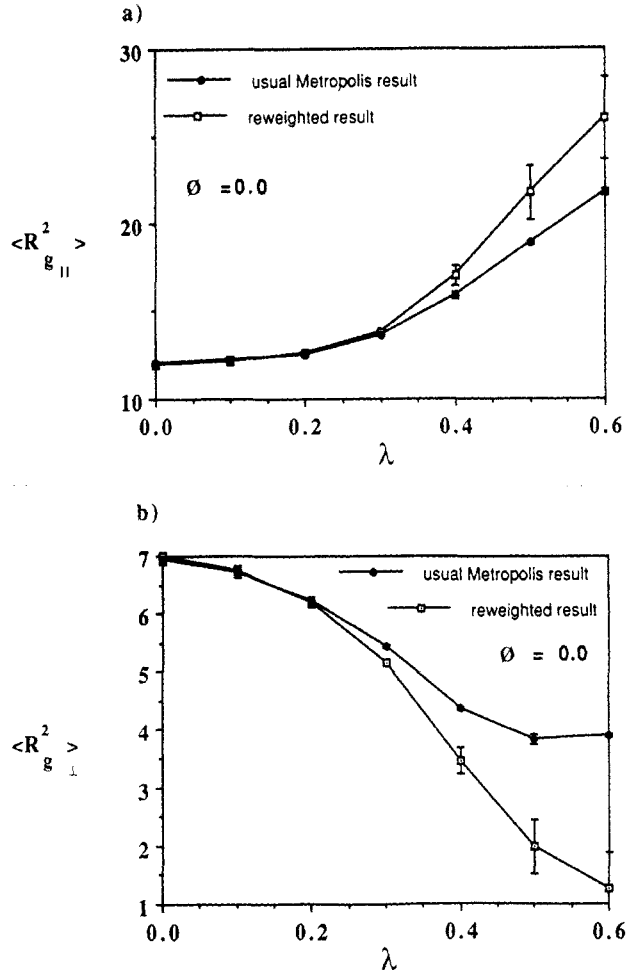

Figure 13. Exact (solid symbols) and approximate (open symbols) results for (a) $\langle R_g^2 \rangle_\parallel$ and (b) $\langle R_g^2 \rangle_\perp$ for $\phi = 0$ and $\lambda_1 = 0.2$ (see eqs 6 and 7). Error bars are as in Figure 9.

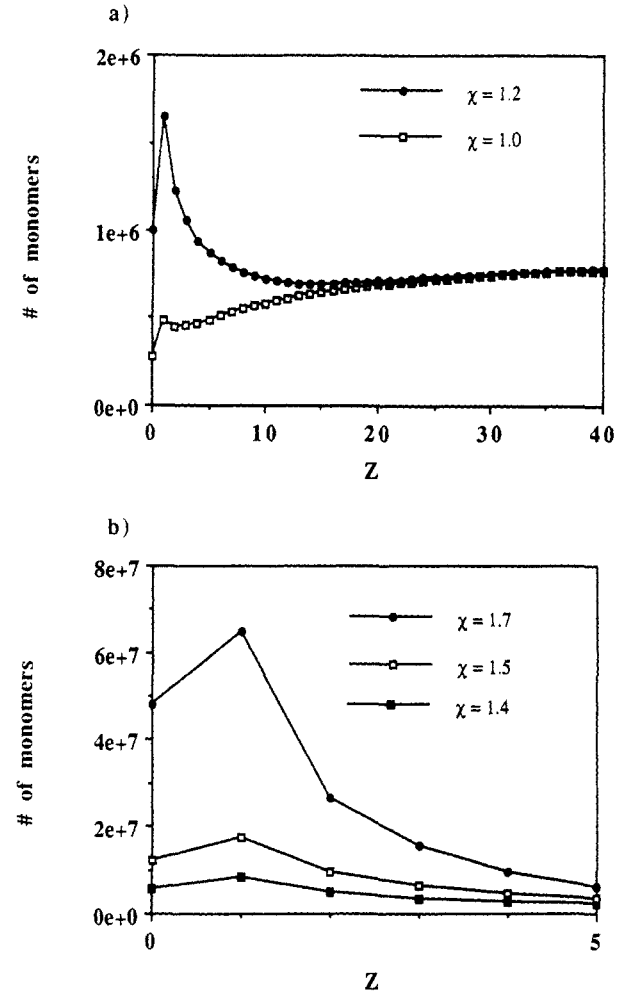

Figure 14. Monomer distribution for homopolymer ($N = 50$) with respect to the wall at $Z = 0$ for (a) $\chi = 1.0$ and 1.2 and (b) $\chi = 1.4$, 1.5, and 1.7. Note the change of scale required because of the high concentration near the surface.

depending on the property being averaged, the statistical quality remains high and the agreement with the direct calculation at λ_2 is excellent. For larger differences in λ_1 and λ_2 the approximate value sometimes deviates significantly from the nonreweighted value and the standard deviation of the average becomes quite significant. This "interpolation" scheme provides a large savings in computer time for a more accurate estimation of the ϕ and λ dependence of conformational properties.

3.2.3. Homopolymer Equilibrated at a Solid Surface. Figure 14 shows the monomer distribution profiles for a nongrafted homopolymer of length 50 for various values of χ. The energetic parameter, χ, has the same meaning as described in section 2.5, with all monomers being of type B. The surface excess can be computed analogously to the representation in Figure 7. From Figure 15 one can estimate that at $\chi = 1.18$ the surface excess is approximately zero. For $\chi < 1.18$ there is a decrease in monomer density near the solid surface, as expected on entropic grounds.[23,24] Above this χ value, the monomer distribution becomes slightly narrower and the surface excess grows approximately exponentially. It should be kept in mind in comparing these distributions that the total number of monomer units distributed over Z from 0 to 200 is constant. (The large number of "monomer units" is the result of the large number of conformations generated to produce the distribution profile, see section 2.4.)

3.2.4. Copolymer. Figure 16 shows the monomer distribution profiles for a diblock copolymer ($N = 50$) at a relatively low χ value ($\chi = 1.0$). There is surface depletion due to entropy effects, similar to the homopolymer case. The surface depletion qualitatively resembles that predicted by Marques and Joanny.[25] As χ is increased, more polymer is adsorbed to the surface, eventually leading to surface excess.

Figure 17 shows the monomer distribution profiles for a diblock copolymer ($N = 50$) at $\chi = 1.8$, which displays a clear surface excess. The profiles resemble those calculated from self-consistent field methods for a higher density of polymers at a surface.[26] The B monomer distribution resembles that of an adsorbed homopolymer, and the A monomer distribution resembles that of an end-grafted chain with a low adsorption energy (see Figure 12).

Figure 18a shows the monomer distribution profiles for the alternating copolymer at $\chi = 1.0$. Here there is surface depletion, but the presence of the surface clearly seems to exert an influence on the copolymer because of the correlation between A and B groups. Figure 18b shows the monomer distribution profiles for the alternating copolymer at $\chi = 1.6$. The distribution resembles that of Figure 3, with the profile truncated at the surface.

Figure 19a shows $\Gamma_A/[A]$ as a function of χ for the diblock and alternating copolymers of length 50 at the wall. Figure 19b shows the same plot on a logarithmic scale for the values in which $\Gamma_A/[A] > 0$. The χ values for $\Gamma_A = 0$ can be estimated to be 1.51 and 1.28 for the diblock and alternating cases, respectively. Unlike the case of a liquid–liquid interface, the alternating copolymer is preferentially

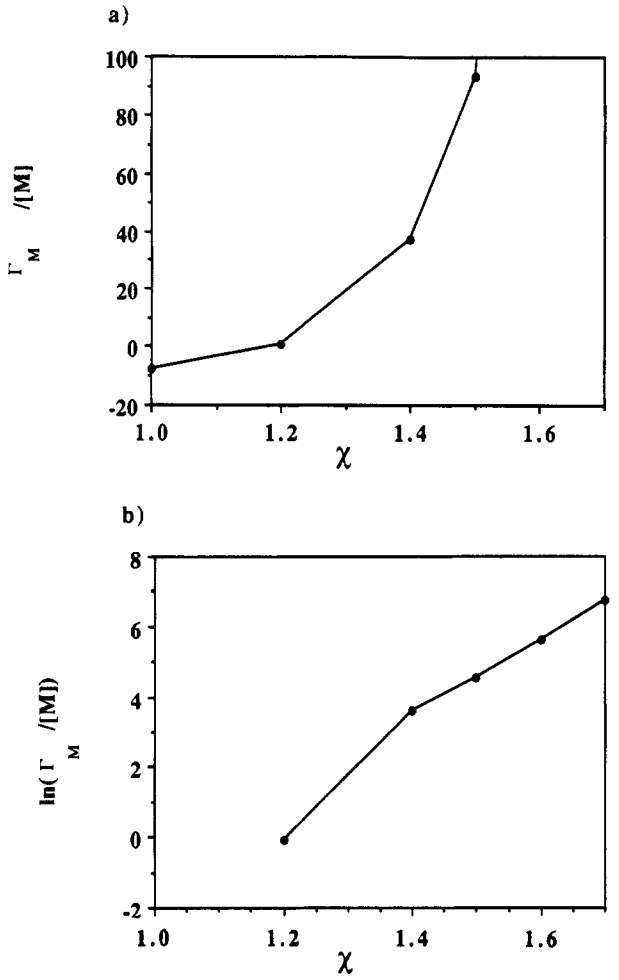

Figure 15. (a) Linear plot of $\Gamma/[M]$ as a function of χ for a homopolymer ($N = 50$). (b) Semilogarithmic plot of $\Gamma/[M]$ for the case of a surface excess.

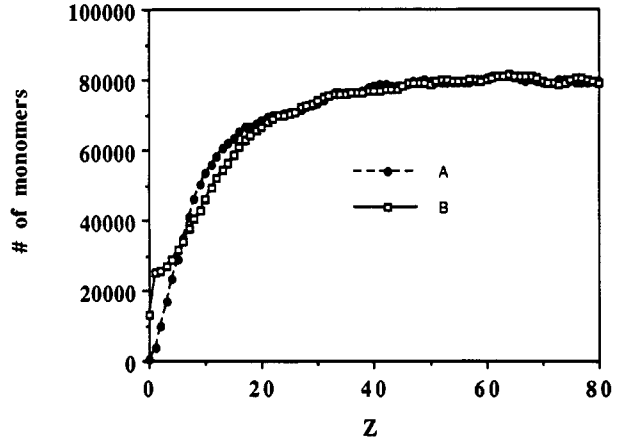

Figure 16. Monomer distributions for a diblock polymer ($N = 50$) with respect to the wall at $Z = 0$ for $\chi = 1.0$.

adsorbed at the solid–liquid interface relative to the diblock.

4. Conclusions and Summary

Initially these calculationes were undertaken to enhance our interpretation of photophysical experiments on polymers at interfaces because most theories or calculations do not present some of the information of interest to us (e.g., number of nonbonding segmental contacts, fraction of monomers in each phase, end-to-end separation, etc.). We have found the pivot algorithm to be very efficient for simulation of isotropic solutions,[13] and so far as we know, the present paper is the first application of this method

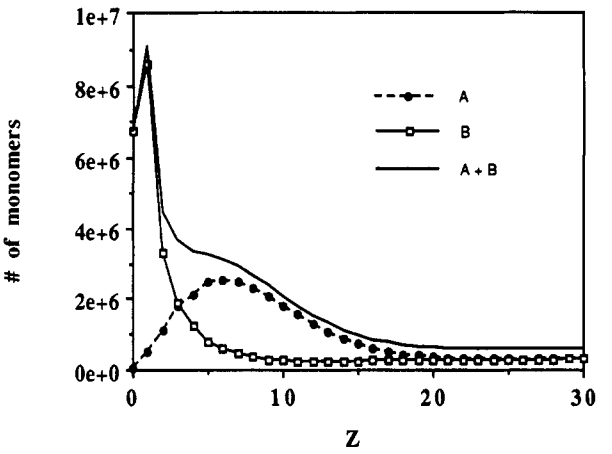

Figure 17. Monomer distributions for a diblock polymer ($N = 50$) with respect to the wall at $Z = 0$ for $\chi = 1.8$.

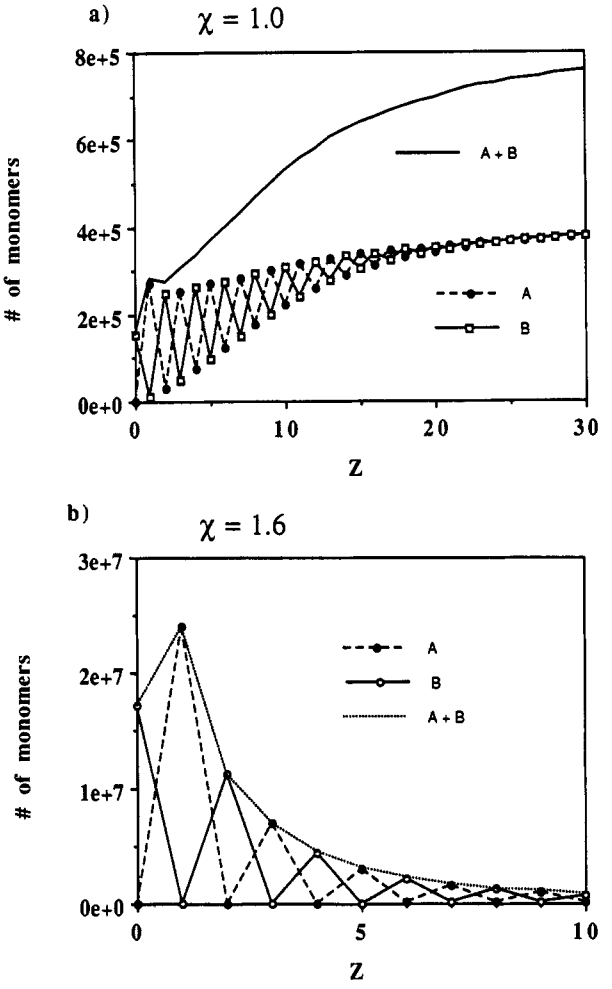

Figure 18. Monomer distributions for alternating copolymers ($N = 50$) with respect to the wall at $Z = 0$ for (a) $\chi = 1.0$ and (b) $\chi = 1.6$.

to polymers at liquid–liquid or solid–liquid interfaces. The method seems to be very efficient for relatively short polymers at infinite dilution. On the basis of our experiments with collapsed polymers in isotropic solution, we believe that this method can be applied to polymers in the weakly overlapping concentration region, but this has not yet been implemented.

The cases studied here are simplified, especially with respect to the energetic symmetry of the two monomer types with respect to the immiscible solvents or the surface–solvent energetic parameter. For real copolymers a larger number of energetic parameters will be required for each monomer in each solvent and for all combinations

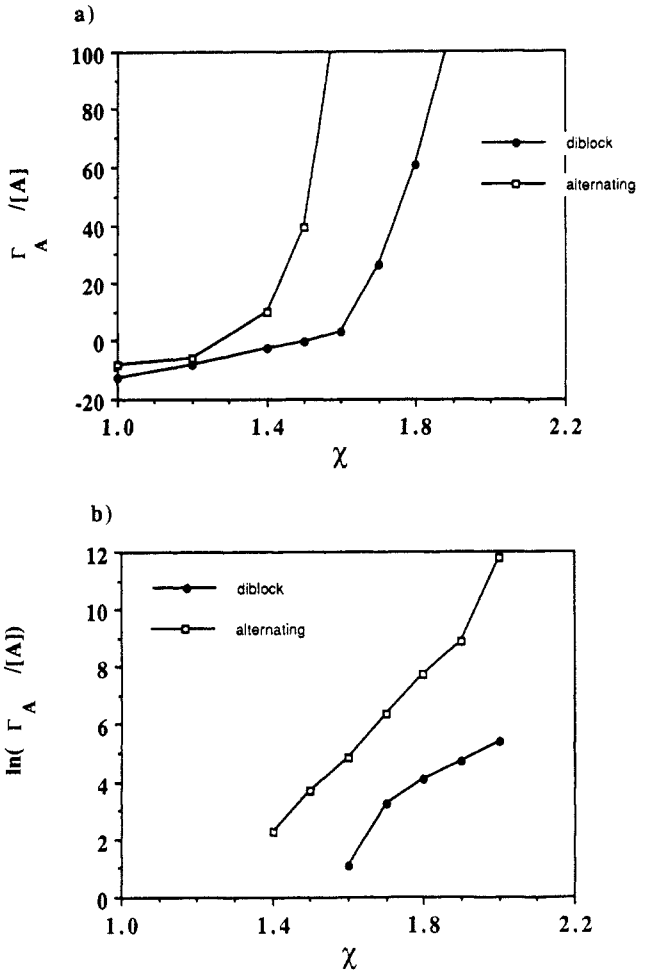

Figure 19. (a) Linear plot of $\Gamma_A/[A]$ for the diblock and alternating copolymers as a function of χ. (b) Semilogarithmic plot of $\Gamma_A/[A]$ for the diblock and alternating copolymers as a function of χ in the case of a surface excess.

of monomer interactions (at least 10 parameters for a copolymer–two solvent system in the most general case). However, for a specific choice of parameters the present method can be applied in a straightforward way, providing an opportunity to predict some complex and nonintuitive structure–property relationships.

The specific conformational and distributional conclusions derived from the present study are not particularly surprising. For the liquid–liquid case a diblock polymer is predicted to be adsorbed at the interface more strongly than an alternating polymer. The opposite is found for the solid–liquid case. For a solid–liquid interface there is a χ value at which the monomer profile switches from a surface deficiency to a surface excess, and the properties of the distribution profile change dramatically at this χ value. The critical χ value is different for a diblock and an alternating polymer, as might be expected.

The case of an end-grafted homopolymer was also considered, in this case with different energetic parameters for segment–segment and segment–surface interactions. The primary goal of this work was to understand the interplay between solvent and surface on polymer conformation. The most important conclusions are the following: (1) The solvent continues to strongly influence intersegmental contacts even for strongly adsorbed polymers, and in fact, the degree of adsorption has very little effect on this property. (2) As the polymers were strongly adsorbed, the end-to-end distance increases significantly, primarily for $\lambda > 0.3$. (3) For $\lambda < 0.2$ there is very little effect on the polymer because the ellipsoidal polymer tends to orient itself to provide the maximum contact with the surface, while for $\lambda > 0.3$ the polymer begins to be flattened out into a more two-dimensional structure. We note that for high ϕ (compact coil) and high λ (strongly adsorbed coil) the pivot algorithm begins to become less efficient because of the large number of coil self-intersections and the difficulty in satisfying the Metropolis criterion (see Table I).

Acknowledgment. This research was supported by a grant from the National Science Foundation Polymers Program (DMR-9000562) and the Robert A. Welch Foundation (F-356). We acknowledge the contribution of K. R. Dean to the earlier stages of some of this work and Dr. G. Grest (Exxon Research and Engineering) for his comments. S.E.W. acknowleges a useful conversation with Prof. G. Zifferer (University of Vienna) concerning this work.

References and Notes

(1) Halperin, A.; Tirrell, M.; Lodge, T. P. *Adv. Polym. Sci.* **1991**, *100*, 31 and references contained within.
(2) Milner, S. T. *Science* **1991**, *251*, 905 and references contained within.
(3) Balazs, A. C.; Siemasko, C. P.; Lantman, C. W. *J. Chem. Phys.* **1991**, *94*, 1653.
(4) Cosgrove, T.; Finch, N. A.; Webster, J. R. P. *Macromolecules* **1990**, *23*, 3353.
(5) Halperin, A.; Pincus, P. *Macromolecules* **1986**, *19*, 79.
(6) Madras, N.; Sokal, A. D. *J. Stat. Phys.* **1988**, *50*, 109.
(7) McCrackin, F. L. *J. Chem. Phys.* **1967**, *47*, 1980.
(8) Lal, M.; Stepto, R. F. T. *J. Polym. Sci., Polym. Symp.* **1977**, *61*, 401.
(9) Wall, F. T.; Mandel, F.; Chin, J. C. *J. Chem. Phys.* **1976**, *65*, 2231.
(10) Bellemans, A.; Orban, J. *J. Chem. Phys.* **1981**, *75*, 2454.
(11) Rubin, R. J. *J. Chem. Phys.* **1965**, *43*, 2392.
(12) Eisenriegler, E.; Kremer, K.; Binder, K. *J. Chem. Phys.* **1982**, *77*, 6296.
(13) Byers, J. D.; Parsons, W. S.; Webber, S. E. *Macromolecules* **1992**, *25*, 5935.
(14) Johnson, L. A., et al. *J. Chem. Phys.* in press.
(15) Metropolis, N.; Rosenbluth, A. W.; Rosenbluth, M. N.; Teller, A. H.; Teller, E. *J. Chem. Phys.* **1953**, *21*, 1087.
(16) Balazs and co-workers have recently considered alternating polymers at interfaces. (a) Yeung, C.; Balazs, A. C.; Jasnow, D. *Macromolecules* **1992**, *25*, 1357. (b) Li, W.; Yeung, C.; Jasnow, D.; Balazs, A. C. *Macromolecules* **1992**, *25*, 3685. In the latter reference it is proposed that an alternating polymer becomes localized at an interface for $\chi \geq 0.4$, on the basis of their Figure 5 and for equal energetic penalties for the monomer being in the "wrong" solvent. This is consistent with our calculations (see Figure 8 and later discussion).
(17) Dean, K. R.; Webber, S. E. In *Physics of Polymer Surfaces and Interfaces*; Sanchez, I., Ed.; Manning Publications: Greenwich, CT, 1992; p 285.
(18) We define these quantities such that $\langle R_g^2 \rangle = \langle R_g^2 \rangle_\parallel + \langle R_g^2 \rangle_\perp$.
(19) Hahn, T. D.; Kovac, J. *Macromolecules* **1990**, *23*, 5153.
(20) Note that there must be at least one contact at the polymer terminus, so $(C_w)_{min} = 0.02$.
(21) McCrackin, F. L. *J. Chem. Phys.* **1967**, *47*, 1980.
(22) Rubin, R. J. *J. Chem. Phys.* **1965**, *43*, 2392.
(23) Asakura, S.; Oosawa, F. *J. Chem. Phys.* **1954**, *22*, 1255.
(24) Joanny, J. F.; Leibler, L.; de Gennes, P.-G. *J. Polym. Sci.* **1979**, *17*, 1073.
(25) Marques, C. M.; Joanny, J. F. *Macromolecules* **1990**, *23*, 276.
(26) Evers, O. A.; Sheutjens, J. M. H. M.; Fleer, G. J. *Macromolecules* **1990**, *23*, 5221.